Oxidation of Metals, Vol. 25, Nos. 3/4, 1986

Cyclic Oxidation Behavior of Ni_3Al–0.1B Base Alloys Containing a Ti, Zr, or Hf Addition

Shigeji Taniguchi* and Toshio Shibata*

Received May 16, 1985; revised June 5, 1985

Ni_3Al and Ni_3Al-0.1B, with and without additions of about 2% Ti, Zr, or Hf were subjected to a thermal cycling oxidation test in pure flowing oxygen at atmospheric pressure at temperatures cycled between 400 and 1300 K. The scales formed on Ni_3Al and Ni_3Al-0.1B spalled repeatedly, resulting in a considerable mass loss of the specimen. The Ti addition to Ni_3Al led to a repeated scale spallation, whereas Ti added to Ni_3Al-0.1B resulted in a very adherent scale, although the oxidation kinetics were linear and the formation of deeply penetrating Al_2O_3 along the alloy grain boundaries took place. The scales were very adherent on alloys containing Zr and Hf. This was attributed to the so-called keying mechanism, because uneven penetration of Al_2O_3 into the alloy took place, leading to irregularly shaped scale/alloy interfaces. ZrO_2 and HfO_2 particles were incorporated into the Al_2O_3 layer and protrusions, and some of them were formed ahead of the Al_2O_3. The shape of these particles was not stringerlike as found with other alloys. The Ti, Zr, and Hf additions tended to decrease the density of voids formed at the scale/alloy interface, but the extent of the change seems to be insufficient to support the vacancy-sink mechanism. The Hf addition was found to be most effective in forming a protective scale.

KEY WORDS: Ni_3Al; Ni_3Al-0.1B; cyclic oxidation; scale adherence; additive; titanium; zirconium; hafnium.

INTRODUCTION

It has been shown[1-3] that the intermetallic compound Ni_3Al (γ' phase) has high strength at elevated temperatures with a characteristically positive

*Department of Metallurgical Engineering, Faculty of Engineering, Osaka University, Suita, Osaka 565, Japan.

0030-770X/86/0400-0201$05.00/0

temperature dependence of strength over a certain temperature range. The high-temperature strength of Ni-base superalloys is exclusively dependent upon the amount of precipitates consisting primarily of Ni_3Al.[4] Nevertheless, Ni_3Al has not been considered as an engineering material because of its poor ductility at low temperatures. However, it has been shown recently[5] that the addition of a small amount of B (0.05 or 0.1%) to Ni_3Al remarkably improved its room-temperature ductility. Therefore, such materials can be considered as candidates for structural materials at elevated temperatures. B was also found[6,7] to prevent oxygen penetration along grain boundaries of Ni-base superalloys.

The effects of alloying additions on the mechanical properties of Ni_3Al at temperatures up to about 1300 K have been well studied, but much less information is available on its oxidation[8,9] and hot-corrosion[10] behavior. Further, Ni_3Al is recognized as a constituent of directionally solidified eutectic alloys.[11-13]

The examination of the oxidation or hot-corrosion behavior of Ni_3Al containing a small amount of B is, hence, of great interest. The good adherence of a protective scale to the substrate is a fundamental prerequisite for heat-resisting alloys and this has been obtained by the use of small additions of active elements. Among those, Y has been extensively studied,[8,14-18] as have other rare-earth elements.[14,17,18] The present study deals with an attempt to improve the oxidation resistance of Ni_3Al-0.1B base alloys by the addition of Ti, Zr, or Hf. The B-free alloys are also included for comparison.

EXPERIMENTAL PROCEDURES

The alloys were prepared by melting high-purity metals and a Ni-15.5B alloy in a vacuum-induction furnace, followed by casting into a steel die. After an homogenization treatment of the ingots at 1500 K for 172.8 ks (48 hr) in an argon atmosphere, coupon specimens measuring $15 \times 13 \times 1$ mm were cut. The chemical compositions of the alloys are shown in Table I together with their microhardness values.

Alloys 1 to 4 contain 0.09% or 0.1% B, while alloys 5 to 8 are B free. The hardness data clearly show that the B addition increased the hardness by about 50~60%.

As far as the examination with X-ray diffraction and optical microscopy shows, all the alloys were single-phase γ', except alloy 3, which consisted of γ' and γ. However, this does not necessarily mean that all the additives are in complete solution. Ti is soluble in a form of $Ni_3(Al, Ti)$, while B and Zr were reported to be present at grain boundaries,[19] and Hf is soluble in γ phase in Ni-base superalloys. Further study is necessary for a detailed

Table I. Chemical Composition (mass %) and Microhardness (Vickers) in MPa of the Alloys

No.	Ni	Al	B	Ti	Zr	Hf	H_v (load 4.9 N)
1	85.5	14.4	0.09	<0.01			2200
2	84.0	14.3	0.09	1.61			2590
3	86.5	11.2	0.10	<0.01	2.2		2770
4	83.3	14.5	0.10	<0.01		1.92	2290
5	86.6	13.4	<0.001	<0.001	0.005	<0.001	1390
6	84.8	12.9	<0.001	2.36	<0.001	<0.001	1850
7	84.2	13.7	<0.001	<0.001	2.06	<0.001	1740
8	84.7	13.3	<0.001	<0.001	0.025	1.93	1480

specification of the state of the additives, because there is a possibility of forming precipitates of various intermetallic compounds.[7,19,20]

Each coupon specimen consisted of columnar grains of typically 1 × 5 mm and equiaxed grains of 2 ~ 3 mm, while alloy 3 has grains of ~0.5 mm. However, no appreciable difference in the oxidation characteristics between areas of these two kinds of grains was observed. The specimen surface was abraded on successively finer silicon carbide papers up to No. 1200, then polished on a polishing cloth impregnated with alumina polishing powder of 0.3 μm. The final cleaning was performed ultrasonically with acetone and ethanol.

The oxidation runs in flowing, purified oxygen at atmospheric pressure were carried out in an infrared-ray-image furnace equipped with a program controller providing a stable thermal cycle, the temperature pattern of which is shown in Fig. 1. Heating and cooling between 400 and 1300 K took place in 900 s, and the holding time at 1300 K was 3.6 ks. After every 30 cycles the specimens were cooled to room temperature for the mass measurement and visual inspection. The specimens oxidized for specified cycles were examined with X-ray diffraction, optical and scanning electron microscopy, and EPMA.

RESULTS

Kinetics

Figure 1 shows the mass change per unit area of the original specimen (ΔMA^{-1}) plotted against the number of cycles for alloys 1 to 4. Duplicate runs were performed for showing the reproducibility. The numbers in the figure correspond to the alloy number.

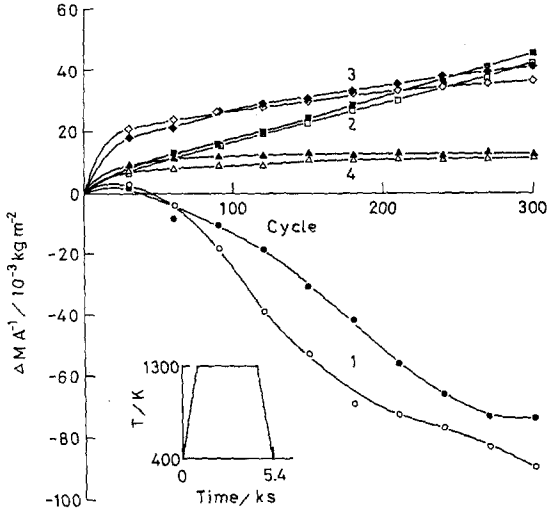

Fig. 1. Mass change per unit area during cyclic oxidation of alloys 1 to 4 in pure flowing oxygen at atmospheric pressure. The temperature cycle is also shown.

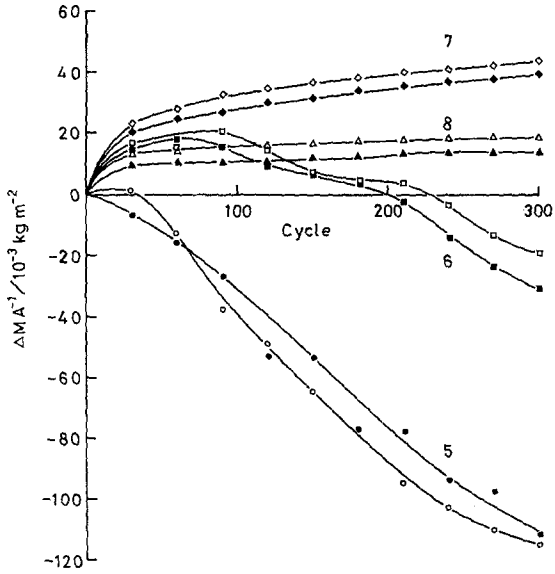

Fig. 2. Mass change per unit area during cyclic oxidation of alloys 5 to 8 in pure flowing oxygen at atmospheric pressure.

The scale formed on alloy 1 was adherent for several cycles, then partial spallation occurred during subsequent cycles, resulting in a considerable mass loss. Contrary to this behavior, all the other alloys formed very adherent scales, although the weight-gain kinetics were quite different.

Alloy 2 shows a mass gain which varies almost linearly with the number of cycles, while alloy 3 shows a relatively large mass gain during the first few cycles, after which the mass gain becomes gradually smaller. On the other hand, alloy 4 has a small initial mass gain, and very small mass change then follows, indicating the formation of a very stable or oxidation-resistant scale during the initial period of oxidation.

Figure 2 similarly shows the kinetics results of alloys 5 to 8. Similar behavior can be seen for the alloys containing the same additive except B. However, the scale formed on alloy 6 spalled slightly within a few cycles in sharp contrast with alloy 2. Both of these alloys contained Ti. Alloys 7 and 8 also formed very adherent scales.

Optical Microscopy

Typical features of the scale/alloy interface of specimens oxidized for 30 cycles are shown in Fig. 3, in which (a) to (d) correspond to alloys 1 to 8, respectively. Alloys 1 and 5 showed extensive spallation, and the adherent scales were rarely observed (Fig. 3a and e). The detached scale seen in the figures consisted mainly of NiO. There is no sign of oxide penetration into the alloys. In contrast to this, those alloys which formed adherent scales are associated with the uneven penetration of the oxide, consisting mainly of Al_2O_3, resulting in irregularly shaped scale/alloy interfaces (Figs. 3b–d, g, and f). In general, the adherent scales consisted of outer NiO, intermediate $NiAl_2O_4$ and innermost Al_2O_3 layers, and occasional protrusions of Al_2O_3 extended from the innermost Al_2O_3 layer into the substrate.

The Ti-containing alloys formed relatively deep Al_2O_3 penetrations along the alloy grain boundaries (Fig. 3b and f) after a large number of cycles. This occurrence was very limited up to 30 cycles. In the case of Zr- or Hf-containing alloys, the penetrating Al_2O_3 contained ZrO_2 or HfO_2 particles, respectively, and some of these particles were formed ahead of the Al_2O_3.

As the oxidation proceeds, the Al_2O_3 penetration into the Ti-containing alloys became so extensive that the alloy grain boundaries were clearly outlined (Fig. 4a), and the size of ZrO_2 or HfO_2 particles tended to become larger (ZrO_2 particles shown by arrows in Fig. 4b).

Figure 5 shows the EPMA results of alloy 4 oxidized for 300 cycles. The HfO_2 particles (arrows in Fig. 5a) are incorporated in the Al_2O_3 scale and protrusions, and their shape is particulate rather than stringerlike, as observed[9,21] by other researchers.

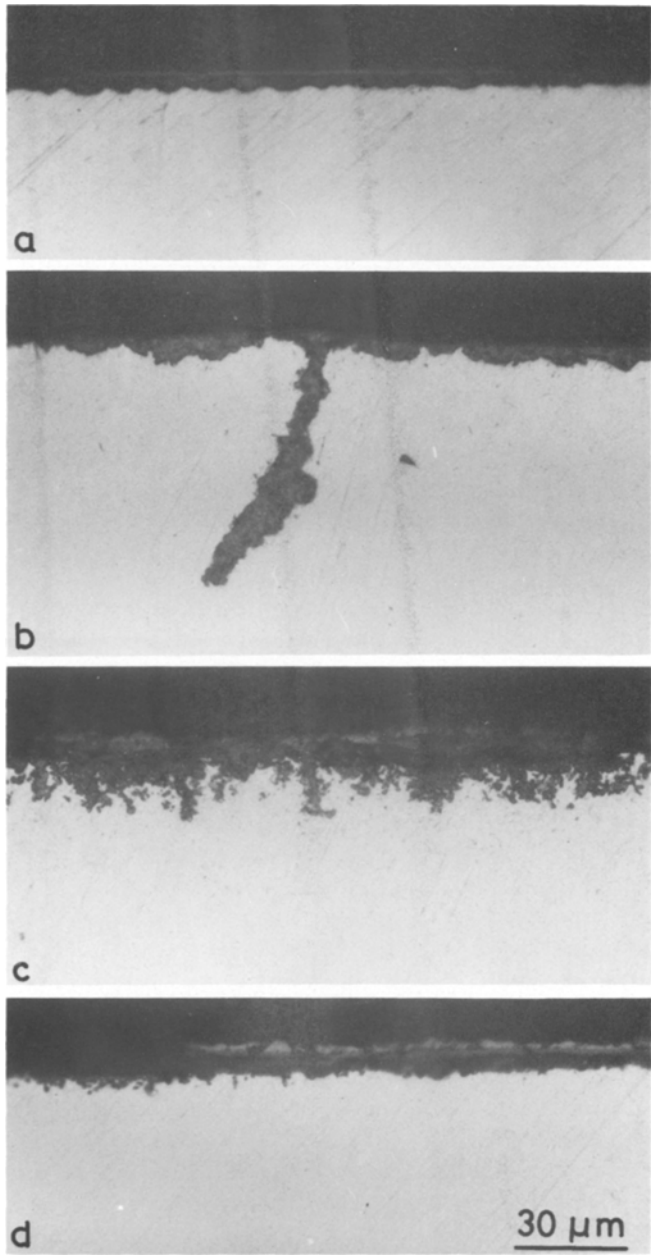

Fig. 3. Scale/alloy interface characteristics of alloys 1 to 8 (a–h, respectively) oxidized for 30 cycles. Adherent scales are associated with uneven penetration of Al_2O_3 layers.

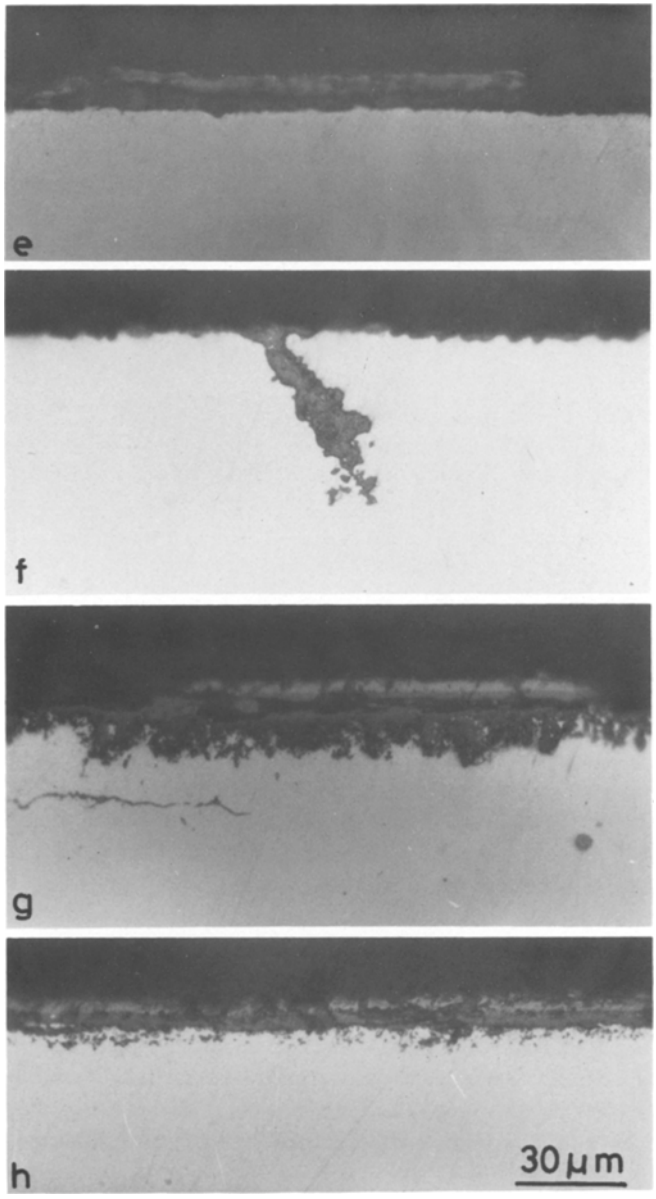

Fig. 3. Continued.

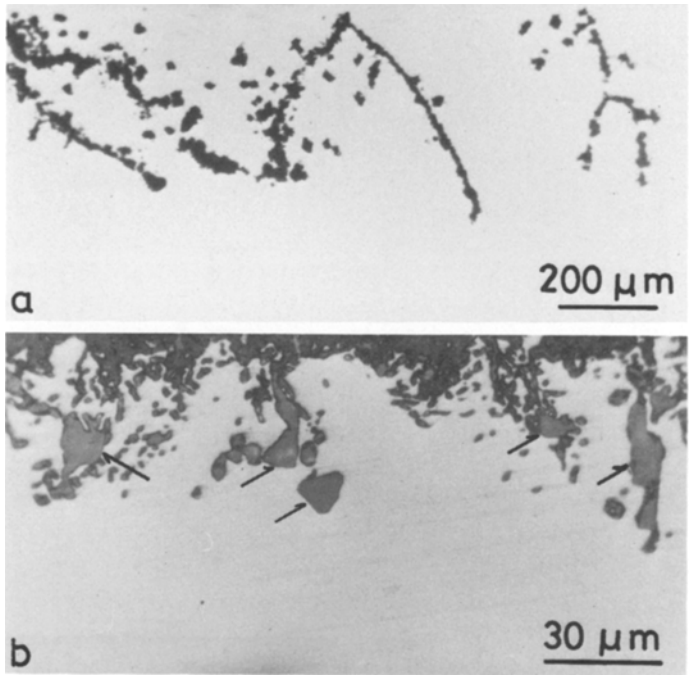

Fig. 4. (a) Deep oxide penetration along the grain boundaries of alloy 2 and (b) relatively large ZrO_2 particles (arrowed) formed ahead of the penetrating Al_2O_3 layer in alloy 3. Both oxidized for 300 cycles.

Other EPMA results showed that there was no sign of TiO_2 formation in the Ti-containing alloys, and Ti was distributed uniformly in Al_2O_3 and in the alloy. Ti is possibly present in the Al_2O_3 as fine $TiAl_2O_5$ particles with a small amount in solution in the Al_2O_3.

SEM Observations

We now describe some characteristic features of the outer surface of the scale and the alloy surface revealed by the scale spallation. The scale on alloy 1 oxidized for 3 cycles was very adherent, but a limited spallation took place over relatively small areas (Fig. 6a). In this case, however, only the outer NiO layer spalled off, and the surface of Al_2O_3 layer beneath it can be seen. This Al_2O_3 layer is not always impermeable to oxygen gas, since a remarkable growth of NiO crystals on the exposed Al_2O_3 layer occurred (Fig. 6b). This may indicate that the Al_2O_3 layer formed up to this period is not completely dense.

In very limited cases, complete spallation to bare alloy took place (Fig. 6c), revealing the alloy surface on which some voids can be seen. However,

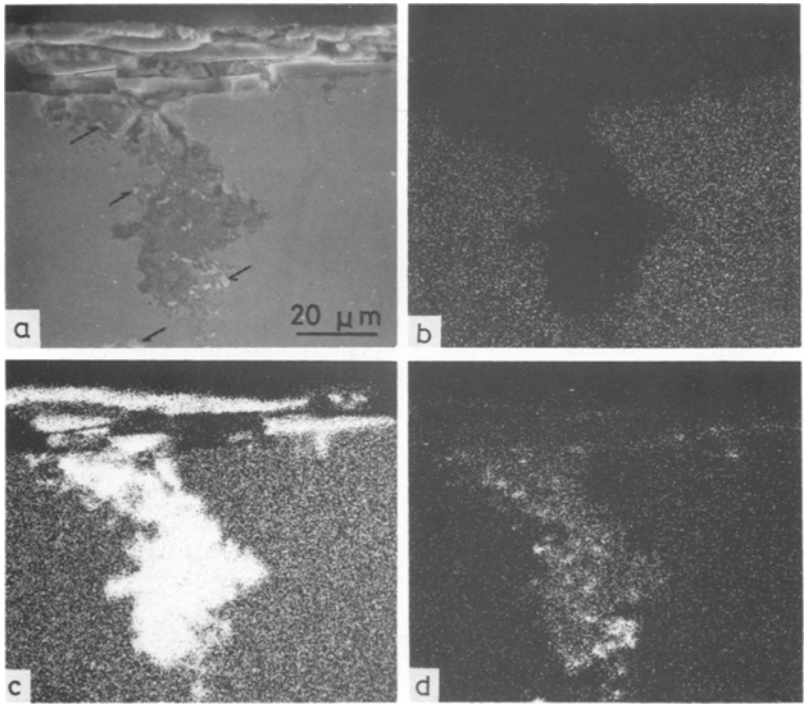

Fig. 5. EPMA results of alloy 4 oxidized for 300 cycles; (a) SEM image showing an Al_2O_3 protrusion with HfO_2 particles incorporated (arrowed) and X-ray images for (b) Ni, (c) Al, and (d) Hf.

alloy 1 oxidized for 30 cycles showed extensive spallation over a wide area (Fig. 7a), and the voided alloy surface was exposed (Fig. 7b). The geometrical shape of the voids are also noteworthy. After this kind of spallation, the growth of NiO is faster on the area where the contact was maintained than on the bottom of the void where the contact was lost earlier (Fig. 7c). This is clearly shown by the results of line analysis of Ni and Al (Fig. 7d). During further oxidation this NiO layer spalls repeatedly, leading to the extensive mass loss as shown in Fig. 1.

When alloy 2 was oxidized, a similar partial spallation of the outer NiO layer covering quite limited areas took place (Fig. 8a), and spallation at the scale/alloy interface was very rare. These tendencies were also observed with alloys 3, 4, 7 (Fig. 8b), and 8, which formed very adherent scales.

In general, the addition of Ti, Zr, and Hf tended to suppress void formation to some degree as can be seen on the bottom of the spalled area (Fig. 9), although this kind of spallation was very rare. On the other hand,

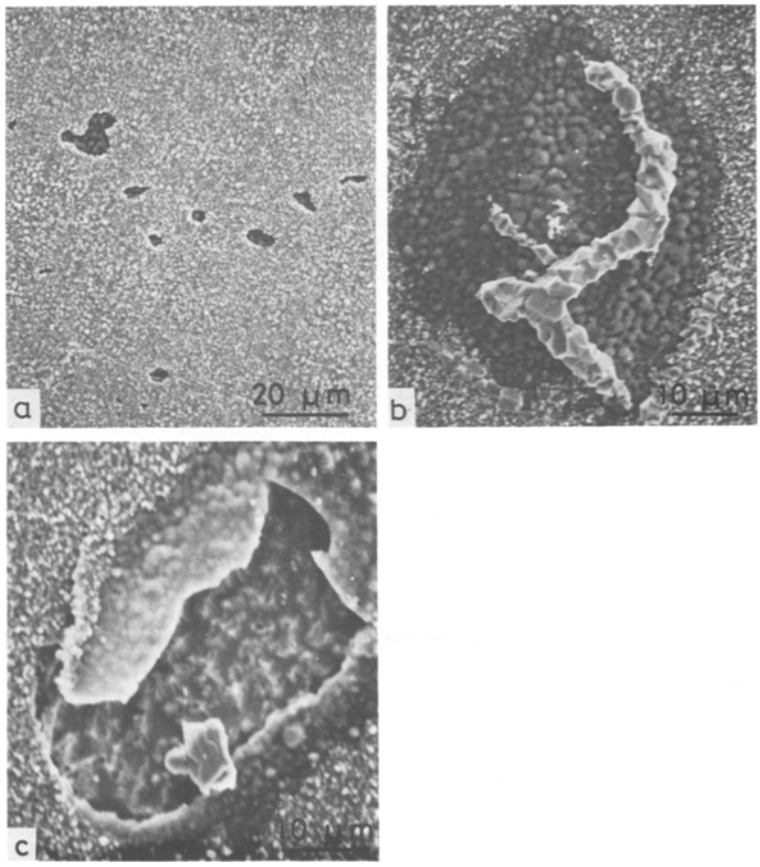

Fig. 6. Alloy 1 oxidized for 3 cycles. (a) Partial spallation of the outer NiO layer and the surface of the Al_2O_3 layer revealed by the spallation; (b) extensive growth of NiO crystals on the Al_2O_3 surface exposed by the spallation of the NiO layer; and (c) partial scale spallation to bare alloy revealing a voided alloy surface.

alloy 5 (pure Ni_3Al) showed extensive spallation even within 3 cycles (Fig. 10a), and this spallation continued with increasing cycles (Fig. 10b). The shape and number of the voids varied from grain to grain. Alloy 6 also experienced partial spallation within 3 cycles, Fig. 11a, and the void formation beneath the scale is seen in Fig. 11b.

DISCUSSION

The isothermal oxidation behavior of Ni_3Al in air and in a temperature range 1173–1473 K was studied by Kuenzly and Douglass.[8] They showed that the oxide scale consisted of outer NiO, intermediate $NiAl_2O_4$ (spinel),

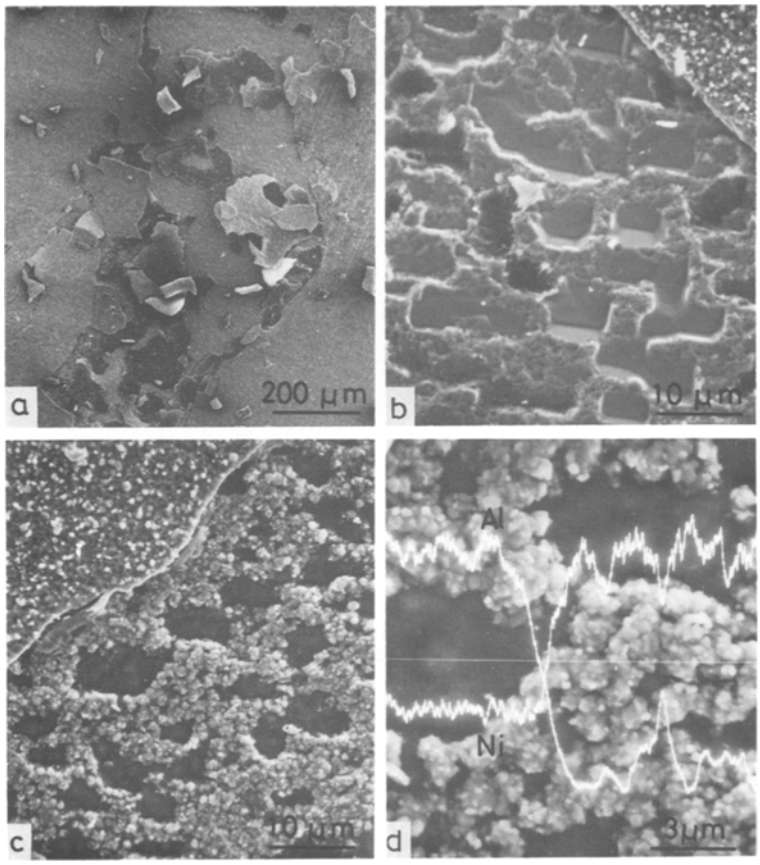

Fig. 7. Alloy 1 oxidized for 30 cycles. (a) Extensive scale spallation; (b) a voided alloy surface revealed by the spallation; (c) preferential NiO growth on the exposed alloy surface; and (d) line analysis of Ni and Al on an area shown in (c).

and inner Al_2O_3 (α-Al_2O_3) layers. As the oxidation proceeds, the NiO layer becomes thinner, while the $NiAl_2O_4$ and Al_2O_3 layers become thicker. The reason for this is that the supply of Ni to the NiO layer is prevented once a dense and continuous Al_2O_3 layer is established, and the $NiAl_2O_4$ layer grows by a solid-state reaction of NiO and Al_2O_3, while Al necessary for the growth of the Al_2O_3 layer is supplied from the alloy. The rate-controlling transport process was found to be the enhanced diffusion of oxygen down the Al_2O_3 grain boundaries.[8]

Similar sequences were also observed by the present authors[22] when alloys 1 and 5 were isothermally oxidized in pure flowing oxygen at atmospheric pressure in the temperature range 1300–1500 K. Fundamentally, the

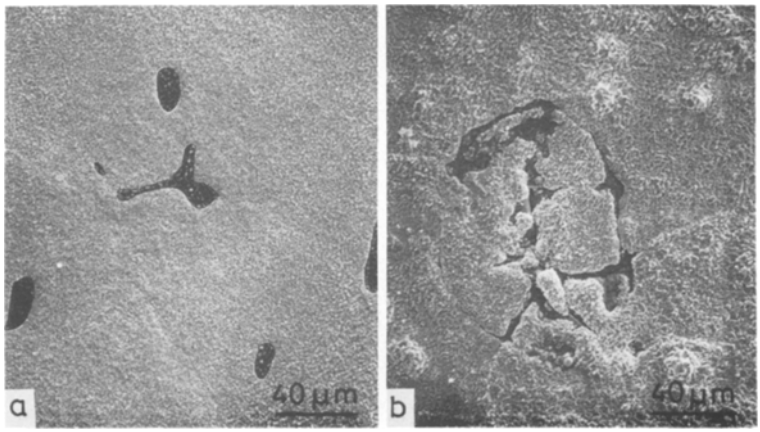

Fig. 8. Limited spallation of the outer NiO layer on (a) alloy 2 oxidized for 3 cycles, and (b) alloy 7 oxidized for 30 cycles.

same sequences were found to take place by X-ray diffraction and metallographic examinations during cyclic oxidation as long as the scales were adherent. However, when the scale spalls to bare alloy, then oxides mainly consisting of NiO form (Fig. 7d), because the alloy surface beneath the Al_2O_3 layer is poor in Al. As the growth of NiO continues, the alloy surface would be enriched with Al, but the next spallation takes place before the enriched Al forms a continuous Al_2O_3 layer.

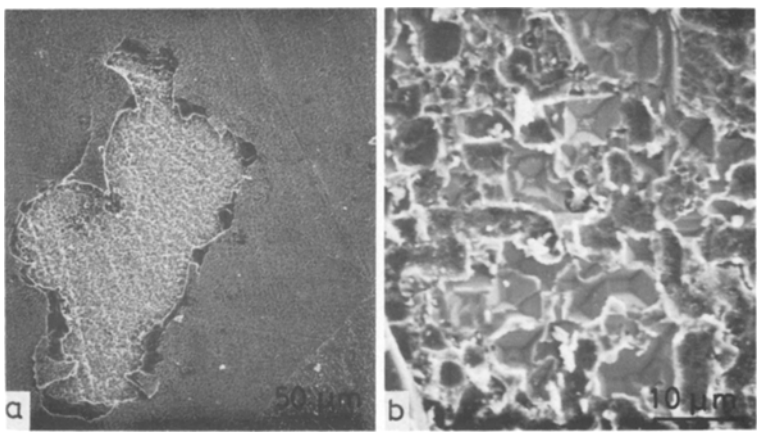

Fig. 9. Alloy 8 oxidized for 30 cycles: (a) limited scale spallation, and (b) a voided alloy surface revealed by the spallation.

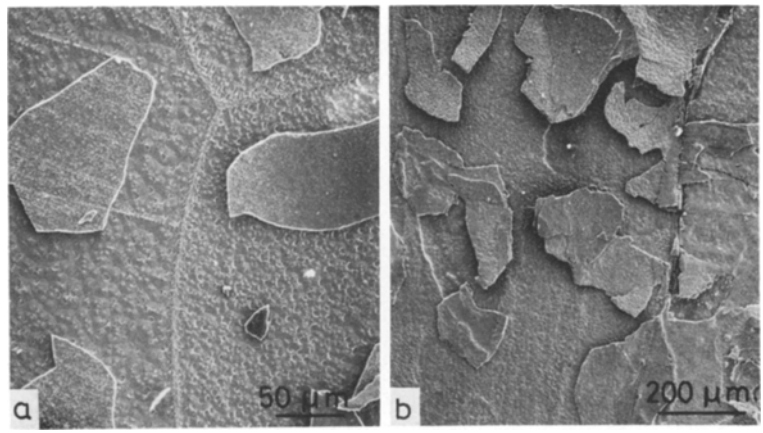

Fig. 10. Extensive scale spallation on alloy 5 oxidized for (a) 3 cycles and (b) 30 cycles.

Another noteworthy feature of the oxidation of Ni_3Al is the extensive void formation on the substrate surface at the scale/substrate interface. This void formation enhances the scale spallation when thermally induced stresses develop. As the isothermal oxidation study[22] on alloys 1 and 5 showed that there was no scale spallation during oxidation at temperature and that the scale spallation took place during cooling, it can be said that the extensive spallation (Figs. 7a and 10) was a result of the temperature change. The order of stress was evaluated.[8] The addition of B to Ni_3Al seems to have almost no influence in this respect.

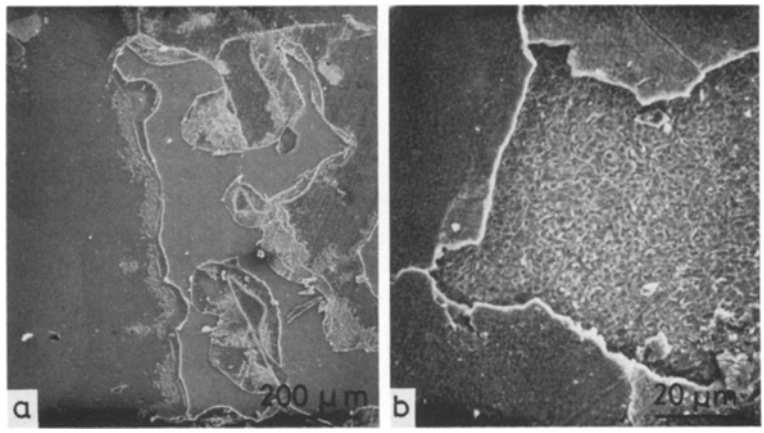

Fig. 11. Alloy 6 oxidized for 3 cycles: (a) extensive scale spallation, and (b) a voided alloy surface revealed by the spallation.

The mechanism of this kind of void formation was presented[8,15] in relation to a Kirkedall effect associated with the growth of Al_2O_3 which involves a preferential consumption of Al in the alloy near the scale/alloy interface.

From the date on alloys 1 and 5 the effect of B addition to pure Ni_3Al, it may be concluded that B improved the scale adherence for the initial few cycles (compare Figs. 6a and 10a), but later extensive spallation takes place on alloy 1, and a protective scale is no longer formed. Thus, the effect of B is quite limited, and it is necessary to find some suitable additive for improving the scale adherence.

When Ti was added together with B, the scale adherence was improved very much, but when Ti was added alone the scale was only partly adherent to the alloy. The partial spallation took place even within 3 cycles. This implies some interaction between Ti and B.

Although adherent scales were formed on alloy 2, the mass gain during oxidation was linear, and this tendency seems to continue more than the period tested in the present study. The penetration of Al_2O_3 along the alloy grain boundaries is also remarkable. These facts may limit the usefulness of this alloy as a structural material, since such oxide penetration decreases the mechanical properties of the alloy a great deal.

The influence of Ti additions is hard to explain at this moment. However, Ikuma and Gordon[23] reported that Ti added to polycrystalline Al_2O_3 together with Mn increased its creep rate by increasing the Al-ion vacancy concentration. Further, Lagrange *et al.*[24] found that the addition of Ti to a Fe-Ni-Cr-Al alloy reduced the oxide growth stress and the stress level in the scale, although the scale adherence was reduced. These findings may indicate that some modification of the mechanical property of the scale, which would vary with or without B, is responsible.

The addition of Zr to Ni_3Al and Ni_3Al-0.1B increased the oxidation rate markedly during the initial cycles (Figs. 1 and 2). This is attributable to an increased rate of Al_2O_3 formation initially (Figs. 3c and g) followed by a decrease in the rate during subsequent cycles by the growth of ZrO_2 particles formed ahead of the penetrating Al_2O_3 (Fig. 4b), which can alter the diffusion of Al. The impoverishment of Al near the scale/alloy interface may also contribute to this when a considerable amount of Al has been consumed. Pandy *et al.*[25] also observed a similar rate increase by the addition of Zr to an Fe-Cr-Al alloy.

Improved adherence by the Zr addition can be explained by the so-called keying mechanism, due to the extensive penetration of Al_2O_3. On the other hand, the vacancy-sink mechanism is unlikely because a considerable amount of voids remained. Another explanation for the beneficial effect of the Zr addition involves the idea that Zr increases the oxide/metal bond

strength.[26] Although this may be feasible, some evidence for this should be given.

The results of the present study indicate that addition of Hf is the most effective, since the oxidation rate was greatly decreased, and the scale adherence was significantly improved. Although a limited partial spallation to bare alloy took place (Fig. 9), no evidence of extensive growth of NiO crystals or a loss of protectivity was observed. This suggests that the Hf addition provided a healing ability when part of the scale was damaged. This healing is possibly performed by enhanced diffusion of Al in the alloy.

Giggins *et al.* attributed improved scale adherence caused by Hf additions to a keying effect of HfO_2 particles protruding into the substrate. Hindam *et al.*[21] and Tsipas[9] observed relatively long HfO_2 particles located between the Al_2O_3 layer and the substrate as if they are "nails" holding the two together. In the present study, however, such HfO_2 "nails" were not observed. The protrusions of Al_2O_3 incorporated with HfO_2 particles (Fig. 5a) were considered to be responsible for the improved scale adherence. Further, the vacancy-sink mechanism seems inapplicable to the present study, because no significant reduction of the interfacial void concentration was noted.

A plausible mechanism suggested for the improved scale adherence involves enhanced scale plasticity,[24,27,28] by which the thermally induced stress as well as the growth stress can be accommodated to some extent. Ti, Zr, and Hf in solution in Al_2O_3 may enhance its plasticity by increasing the Al-ion vacancy concentration. Within the scope of the present results, no detailed discussion can be made on this point.

ACKNOWLEDGMENT

The authors are grateful to Central Research Laboratories, Sumitomo Metal Industries, Ltd. for the chemical analysis of the specimen alloys.

REFERENCES

1. R. G. Davies and N. S. Stoloff, *Trans. Met. Soc. AIME* **233**, 714 (1965).
2. O. Noguchi, Y. Oya, and T. Suzuki, *Met. Trans.* **12A**, 1647 (1981).
3. N. S. Stoloff, *Int. Met. Rev.* **29**, 123 (1984).
4. N. Yukawa, *Bull. Japan. Inst. Met.* **11**, 707 (1972).
5. K. Aoki and O. Izumi, *J. Japan Inst. Met.* **43**, 1190 (1979).
6. D. A. Woodford, *Met. Trans.* **12A**, 299 (1981).
7. D. A. Woodford and R. H. Bricknell, *Met. Trans.* **12A**, 1467 (1981).
8. J. D. Kuenzly and D. L. Douglass, *Oxid. Met.* **8**, 139 (1974).
9. D. N. Tsipas, *Trans. Japan Inst. Met.* Supplement 569 (1983).
10. K. Onisawa, M. Chigasaki, and K. Soeno, *Tetsu-to-Hagané* **68**, 130 (1982).
11. K. D. Sheffler, R. H. Barkalow, A. Yuen, and G. R. Leverant, *Met. Trans.* **8A**, 83 (1977).
12. P. R. Bhowal and M. Metzger, *Met. Trans.* **9A**, 1027 (1978).

13. G. C. Wood, F. H. Stott, and J. G. Fountain, *Corr. Sci.* **19**, 441 (1979).
14. J. K. Tien and F. S. Pettit, *Met. Trans.* **3**, 1587 (1972).
15. A. Kumar, M. Nasrallah, and D. L. Douglass, *Oxid. Met.* **18**, 227 (1974).
16. I. M. Allam, D. P. Whittle, and J. Stringer, *Oxid. Met.* **12**, 35 (1978).
17. R. Nemoto, *Bull. Japan Inst. Met.* **18**, 192 (1979).
18. Y. Saito, *Tetsu-to-Hagané* **65**, 747 (1979).
19. R. F. Decker and C. T. Sims, *The Superalloys*, C. T. Sims and W. C. Hagel, eds. (Wiley, New York, 1972), chap. 2, p. 33.
20. A. Baldan and D. R. F. West, *J. Mat. Sci.* **16**, 24 (1981).
21. H. Hindam, J.-J. Hechler, and D. P. Whittle, *Proc. ICMC* (1984), p. 353.
22. S. Taniguchi and T. Shibata, to be published.
23. Y. Ikuma and R. S. Gordon, *J. Mat. Sci.* **17**, 2961 (1982).
24. M. H. Lagrange, A. M. Huntz, and J. H. Davidson, *Corr. Sci.* **24**, 613 (1984).
25. J. L. Pandey, S. Prakash, and M. L. Mehta, *Proc. ICMC* (1984), p. 389.
26. C. A. Barrett, A. S. Khan, and C. E. Lowell, *J. Electrochem. Soc.* **128**, 25 (1981).
27. J. Stringer, *Corr. Sci.* **10**, 513 (1970).
28. S. Taniguchi, *Trans. Iron Steel Inst. Japan* **25**, 3 (1985).